Testing bump in the Cosmological Power Spectrum Using Dwarf Galaxies

Maxim Zabelkin¹, Sergey Drozdov², Oleg Skorikov², and Sergey Pilipenko²

¹Faculty of Space Research, Lomonosov Moscow State University, Leninskie Gory 1, 119991 Moscow, Russia

²P.N. Lebedev Physical Institute RAS, Profsoyuznaya St. 84/32, 117997 Moscow, Russia

November 27, 2025

Abstract

We analyze the possibility of using observational data on nearby dwarf galaxies — their luminosity functions and spatial distributions — to constrain deviations of the cosmological power spectrum from the standard one. Specifically, we consider a cosmological model with a "bump" in the power spectrum at a wavelength of 1.3 Mpc and a dimensionless amplitude $\mathcal{A}=2.0$. Such a spectrum is motivated by observations of an excess number of galaxies at high redshifts. The bump leads to a noticeable increase in the luminosity function in the range $-13 > M_B > -17$ at z=0. Comparison with observations constrains the bump amplitude to $\mathcal{A}<0.25$ at a 3-sigma significance level for a wavelength of 1.3 Mpc. For wavelengths smaller than 0.8 Mpc, the bump manifests only in the luminosity function of dwarfs with $M_B > -14$.

1 Introduction

Currently, the Λ CDM cosmological model is supported by a wide range of observational data. However, there exist several observations that can be interpreted in favor of various extensions to this model. These in-

clude the missing satellites problem [1], the cusp-core problem [2], the Hubble tension [3], and a possible excess of galaxies at high redshifts [4–6]. One of the quantities available for modification in the standard cosmological model is the density perturbation power spectrum. It characterizes the amplitude of

matter density deviations from the mean in the Universe as a function of spatial scale.

According to modern theoretical understanding, initial matter density inhomogeneities arose during inflation, and the simplest form of the initial spectrum is a power law with an index close to 1. However, depending on the inflation model, the spectrum may contain various features [7,8]: "bumps" (peaks at certain scales), changes in the spectral index at some scales, etc. Therefore, measuring the initial power spectrum can test inflation models.

Modern constraints on the power spectrum are summarized in [9]. It is well constrained in the wavenumber range from 2×10^{-4} ${\rm Mpc^{-1}}$ to 2 ${\rm Mpc^{-1}}$ (corresponding to wavelengths approximately 30 Gpc to 3 Mpc). On scales smaller than about 3 Mpc, constraints are weaker, making this range of interest for study. In [10], power spectrum models with a bump were proposed that better describe high-redshift galaxy data from the James Webb Space Telescope than the ΛCDM model. The best-fit model features a bump at scale $k_0 = 4.7 \text{ Mpc}^{-1} (k_0 = 7)$ h/Mpc, where h = 0.67 is the dimensionless Hubble constant), corresponding to a wavelength of about 1.3 Mpc.

The presence of a bump leads to various potentially observable consequences [10–15]. Simple Press-Schechter theory suggests that increasing perturbation amplitude initially increases the number of gravitationally bound objects (halos) in the mass range corresponding to the bump scale, producing a "bump" in the halo mass function. These halos form earlier than in Λ CDM. Over time,

the halo mass function approaches the standard one, smoothing and shifting the bump toward larger masses. If halos formed due to the bump can form stars, this leads to early galaxy formation, affecting galaxy luminosity functions, the rate of reionization, and the 21 cm line signal. Increased numbers of dwarf halos may also affect expected dark matter annihilation signals.

In this work, we examine the bump's effect on dwarf galaxy counts in the nearby Universe at z = 0. Dwarf galaxies have masses up to $3 \times 10^{10} M_{\odot}$, corresponding to the bump scale. The mass-scale relation is given by:

$$M \approx \langle \rho \rangle \left(\frac{2\pi}{k_0}\right)^3,$$
 (1)

where $\langle \rho \rangle$ is the mean matter density of the Universe. Such mass objects should have formed sufficiently early, at $z \geq 8$, corresponding to a Universe age under 1 billion years. The number of galaxies at this epoch was estimated in [10]. Over subsequent billions of years, galaxies underwent complex evolution, including mergers and star formation, not described by simple linear theory. The dark matter halo mass function was also estimated in [10], showing that by today the bump's effect on halo mass function is relatively small — information about the bump is lost: a bump that increased halo counts by 70 times at z = 10 for $3 \times 10^{10} M_{\odot}$ halos only increases counts by a factor of 3 at z = 0. However, in this estimate baryonic evolution was not considered. Measuring virial masses for halos with $3 \times 10^{10} M_{\odot}$ or less is complicated observationally [16], and baryonic processes can make galaxies nearly unobservable

due to low luminosity or surface brightness (e.g., ultra-diffuse galaxies [17]). Thus, a factor of 3 difference in halo counts may be small enough to require further study to determine observability.

Unlike dark matter, which interacts gravitationally only, baryons undergo complex processes currently not fully modeled. These include gas cooling, ionization changes, chemical reactions, magnetic field interactions, star formation, and interactions with stellar radiation. Semi-analytic models, sets of differential equations approximating gas and star evolution based on dark halo growth history, are one approach to include these processes. These equations are based either on simple physical considerations, or approximate the results of detailed simulations.

We use the GRUMPY model [18], which has relatively few equations and an open-source Python code, facilitating understanding and modification. It was designed for dwarf galaxies and excludes processes important for massive galaxies, such as central supermassive black hole effects. [18] shows it reproduces observed dwarf galaxy correlations: mass-size, mass-metallicity, and mass-star formation rate relations. [19] used GRUMPY to constrain the primordial power spectrum, but considered spectra with altered slopes at small scales rather than bumps.

Our main method to test cosmological models with modified power spectra is simulating luminosity functions for dwarf galaxies. Observational data, e.g. from [20], show the dwarf galaxy luminosity function in the Local Volume follows a Schechter function for absolute magnitudes $M_B < -14$, so only mod-

els without strong features in this luminosity range are acceptable.

As a second observational test, we consider the two-point 3D galaxy correlation function (see, e.g., [21]). It is directly related to the power spectrum by Fourier transform, but on ~ 1 Mpc scales, large-scale structure is nonlinear, especially in baryonic galaxy distribution, so the power spectrum derived from the correlation function differs from the initial one. To study the correlation function in the bump model and its difference from the standard spectrum, we compute it for model galaxy samples from GRUMPY. To our knowledge, observed dwarf galaxy correlation functions in the local neighborhood have not vet been obtained, but increasing galaxy samples will enable this.

2 Numerical Dark Matter Halo Models and the GRUMPY Model

We used two numerical models with a cube size of 47 Mpc (= 32/h Mpc) filled with $1024^3 \approx 10^9$ dark matter test particles, particle mass $3.9 \times 10^6 M_{\odot}$. One model used the Λ CDM power spectrum; the other used the $gauss_1$ spectrum from [10] featuring a bump at $k_0 = 4.7$ Mpc⁻¹ (wavelength 1.3 Mpc), bump width $\sigma_k = 0.1$, amplitude A = 20. The power spectrum differs from Λ CDM as:

$$\frac{P_{\text{bump}}(k)}{P_{\Lambda\text{CDM}}(k)} = 1 + A \cdot \exp\left(-\frac{(\log(k) - \log(k_0))^2}{\sigma_k^2}\right).$$
(2)

It is important to note that, despite the fact that (2) has three parameters, for narrow bumps with $\sigma_k \ll 1$, halo mass distributions and evolution depend only on $\mathcal{A} = A\sigma_k$. This can be shown using the Press-Schechter formalism [10,14]. Here, $\mathcal{A} = 2$, required to explain the excess number of galaxies at $z \sim 10$ observed by JWST better than Λ CDM.

Initial conditions were prepared with Ginnungagap code [22]. Simulations were run with public Gadget-2 code [23]. Halo catalogs were extracted using Rockstar [24], selecting halos with mass $> 3 \times 10^8 M_{\odot}$ at simulation end. Merger trees were built tracing the most massive progenitor at each output time. Only the halos traced to z > 0.5 were considered, yielding 600,000 growth histories for the bump model and 1.2 million for Λ CDM.

Figure 1 shows dark matter halo mass functions. The resolution limit is $M > 10^8 M_{\odot}$ (halos with more than 30 particles). The bump's impact on the mass function (discussed in [10]) is evident: a significant increase at z=11 compared to the no-bump spectrum, and a slight increase at z=0 around $10^{11} M_{\odot}$ with a slight decrease below $10^{10} M_{\odot}$.

GRUMPY [18] is a semi-analytic "regulator"-type model with a minimal set of differential equations describing atomic and molecular gas, stars, gas disk size, and metallicity evolution. It accounts for UV background effects (external and stellar), modifying gas accretion rates onto low-mass halos and star formation rates, as well as gas outflows. GRUMPY reproduces various dwarf galaxy relations seen

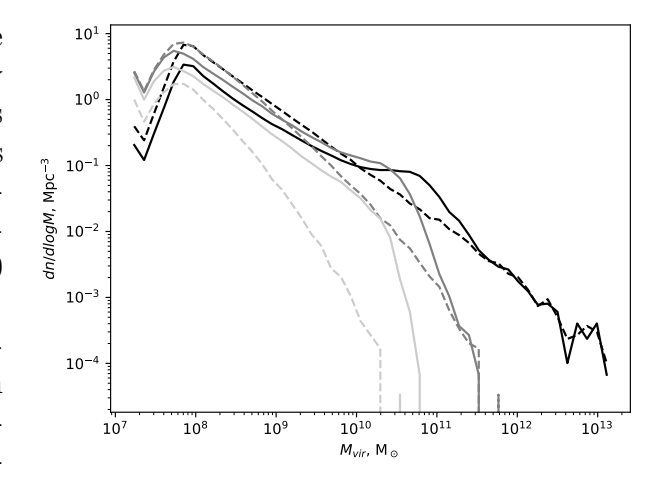


Figure 1: Dark matter halo mass functions at z = 0, 6, 11 (dark to light lines). Solid lines: bump model; dashed lines: Λ CDM.

in hydrodynamic cosmological models and observations.

The model outputs histories of stellar, molecular, and neutral gas masses. Luminosities are computed using star formation rates, assigning a Kroupa initial mass function [25] to new stars, calculating stellar mass distributions at observation time, and then using the FSPS stellar spectra library [26,27] to obtain luminosities in various filters.

3 Dwarf Galaxy Luminosity Function

In the bump cosmological model (2), the number of halos at $z \gtrsim 10$ increases in a certain mass range compared to the standard spectrum. By now, many halos have merged into larger objects. We check how this affects

the observed galaxy number as a function of tor: luminosity.

Figure 2 shows the luminosity functions in the B filter for bump and standard models. At z=0, the bump model yields fewer faint galaxies with $M_B > -13$ than the standard model. Around $M_B \approx -15$, the bump model shows a 3-fold excess compared to the standard, causing a visible kink in the luminosity function.

Observed dwarf galaxy luminosity function in the Local Volume is published in [20]. The sample is complete for $M_B < -14$ and fits a Schechter function well in this range. Figure 2 shows the standard model matches observations well, while the bump model exceeds observational error margins. The χ^2 per degree of freedom for the standard model difference from observations is 1.1 (probability 0.32), while for the bump model it is 14 (probability $\sim 3 \times 10^{-41}$). Thus, the dwarf galaxy luminosity function disfavors a bump with parameters as above at 1.3 Mpc scale.

Correlation Function of 4 Dwarf Galaxies

Besides luminosity, the bump should affect the large-scale structure of galaxies. [11] showed that at high redshifts, the large-scale structure in the bump models differ significantly from the standard spectra. To test bump effects at low redshift, we measure the correlation function ξ for model galaxies with $M_B < -14$ in both models, using the estima-

$$\xi(r) = \frac{DD(r)}{RR(r)} - 1,\tag{3}$$

where DD is the number of galaxy pairs with separations in bin centered at r, and RR is the number of pairs for randomly distributed points in the same bin.

Correlation functions were measured from 200 kpc to 7 Mpc. At very small separations, galaxy pairs cannot exist due to merging. GRUMPY treats halos closer than the virial radius of the larger halo as one halo. Due to the small simulation box size (~ 50 Mpc), the correlation function is distorted for scales larger than $L_{box}/4$, so we limit analysis to smaller scales. The bump scale corresponds to a linear size of 1.3 Mpc, so scales near 1 Mpc are most interesting.

Figure 3 shows that correlation functions for bump and no-bump models are similar. The bump model is about 1.5 times lower at small scales 0.2–0.3 Mpc. For comparison, points show the correlation function for galaxies with $M_B < -20$ from the 2dF catalog [21]. The observed function differs significantly, likely because 2dF galaxies are much brighter and probe larger-scale structures than our models.

To our knowledge, despite catalogs of dwarf galaxies do exist (e.g., [28]), observed dwarf galaxy correlation functions have not yet been obtained, due to difficulties constructing random catalogs that reproduce selection effects.

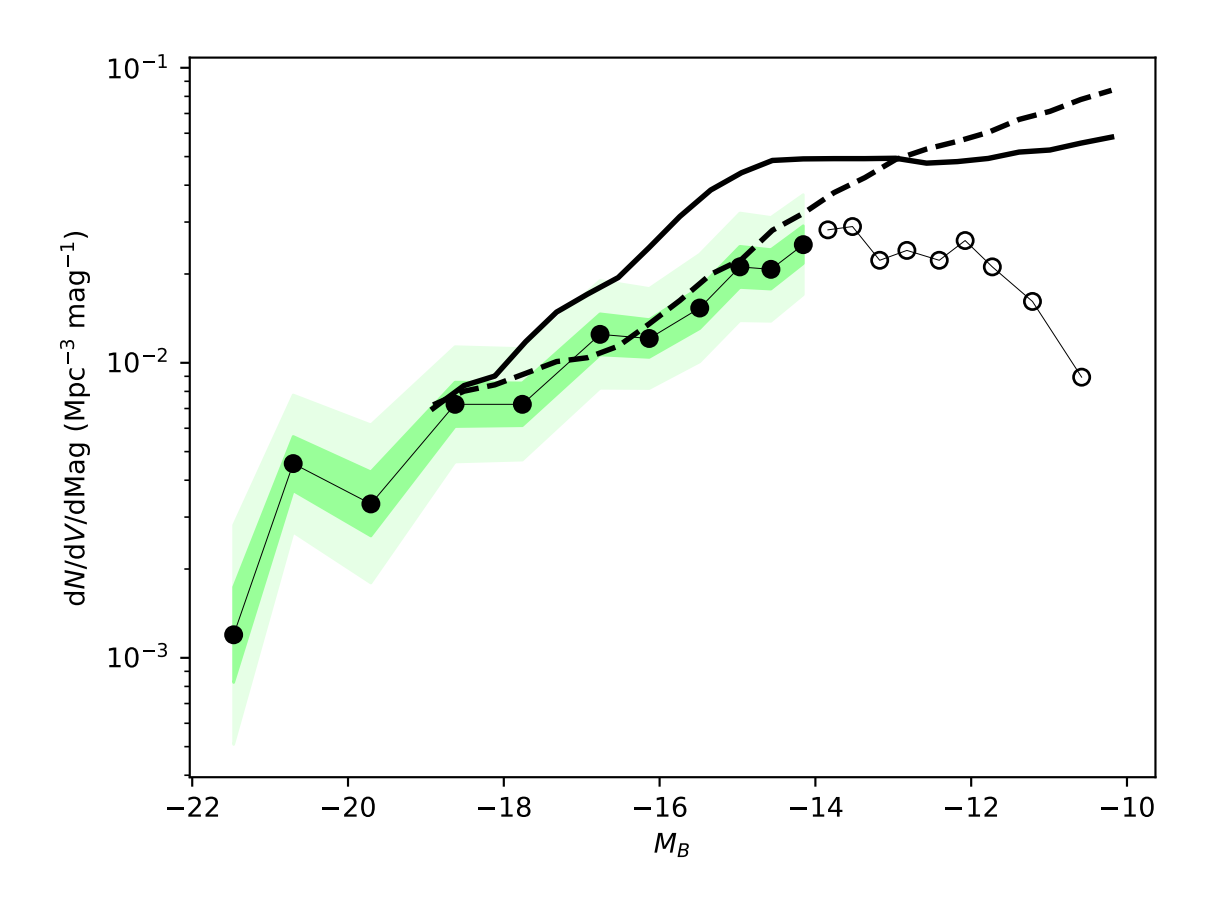


Figure 2: Dwarf galaxy luminosity function in the bump model (solid line) and standard spectrum model (dashed line). Circles show measurements from [20]. Filled circles correspond to $M_B < -14$, where the galaxy sample is complete. Shaded areas indicate Poisson errors at 1σ and 3σ .

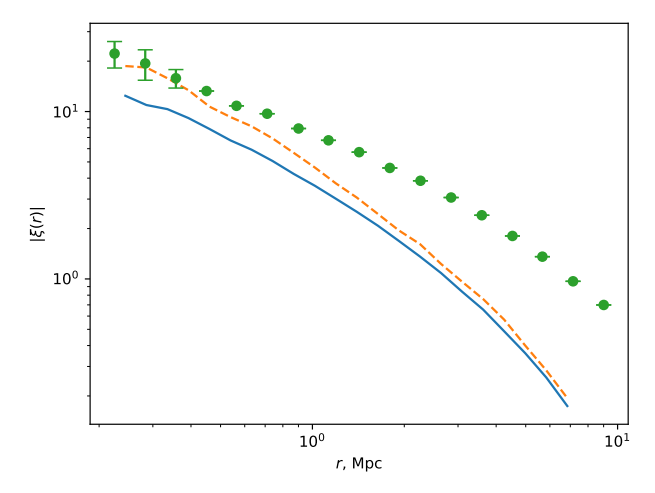


Figure 3: Correlation function of galaxies with $M_B < -14$ in bump (solid line) and no-bump (dashed line) models. Points show measured correlation function from 2dF catalog for galaxies with $M_B < -20$.

5 Observational Constraints on Bump Parameters

The strong distortion of the dwarf galaxy luminosity function at $-17 < M_B < -13$ in the bump model disagrees with observed luminosity functions [20]. Under GRUMPY assumptions, the bump significantly affects stellar masses of present-day galaxies, and a bump at $k_0 = 4.7 \text{ Mpc}^{-1}$ with amplitude $\mathcal{A} = 2$ is ruled out by nearby galaxy observations.

Using observational data, we constrain allowed bump parameters. Numerical modeling on a grid of k_0 , \mathcal{A} is resource-intensive, so we use results from [29], which show small

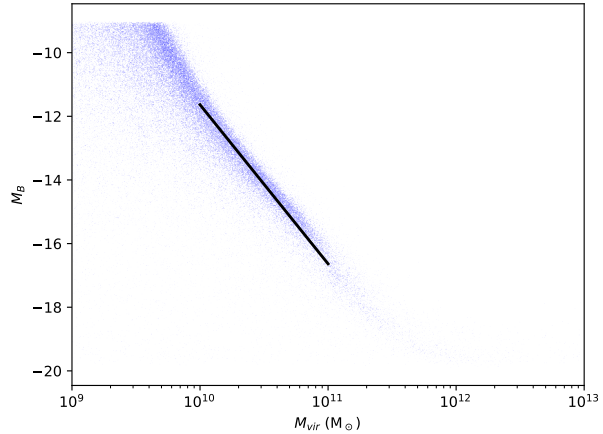


Figure 4: Mass-luminosity relation for galaxies in both models. The line shows $L \propto M_v^2$.

cosmological model variations produce linear changes in halo mass functions. We interpolate our results in parameter space between $\mathcal{A}=2$ and no bump $\mathcal{A}=0$, assuming the luminosity function depends on bump amplitude as:

$$\Phi(M_B; \mathcal{A}) = \Phi(M_B; 0) +
+ \mathcal{A} \frac{\Phi(M_B; 2) - \Phi(M_B; 0)}{2}$$
(4)

Using observed luminosity functions and errors from [20] for $M_B < -14$ (the complete sample), we compute χ^2 and find the probability. With one free parameter \mathcal{A} , the probability exceeds 0.003 (corresponding to 3σ) for $\mathcal{A} < 0.25$, which sets an upper limit on the bump amplitude.

To assess k_0 influence on the luminosity function, we analyze the mass-luminosity relation shown in Fig. 4. It is identical for both models, i.e., independent of the cosmological power spectrum. In the luminosity

range $-17 < M_B < -13$ where the bump appears, luminosity scales as the square of the virial mass. The bump will not contradict observations if this feature shifts to $M_B > -14$, a poorly constrained region observationally. This requires luminosities of galaxies with $M_B = -17$ formed by the bump to decrease by a factor of 16, implying masses decrease by a factor of 4 (from Fig. 4). According to (1), this corresponds to a bump wavenumber $k_0 = 7.4$ Mpc⁻¹ or wavelength 0.8 Mpc. Thus, current observations constrain the bump only for $k_0 < 7.4$ Mpc⁻¹.

The bump effect at smaller wavelengths may be more complex than this estimate, since dwarf galaxies with masses $\lesssim 10^{10} M_{\odot}$ will be part of larger galaxies with $M_B < -14$. Further simulations with different k_0 are needed.

6 Conclusion

We studied dwarf galaxy luminosity distributions in two models: one with the standard initial perturbation spectrum, the other with a bump at 1.3 Mpc wavelength and amplitude $\mathcal{A}=2$ described by (2). Using cosmological simulations to predict dark matter halo distributions and growth histories, we applied the semi-analytic GRUMPY model to compute galaxy luminosities.

The main result — luminosity functions in both models — is shown in Fig. 2. The bump with amplitude $\mathcal{A}=2$ is inconsistent with observations. Interpolating between bump and no-bump models yields an upper limit $\mathcal{A}<0.25$ at 3σ confidence. A slight decrease

in bump wavelength from 1.3 to 0.8 Mpc shifts the luminosity function feature into a poorly constrained observational region. The galaxy correlation function for $M_B < -14$ on scales below 1 Mpc depends on the initial spectrum but has not yet been measured observationally for such galaxies.

Future work includes improving the semianalytic model to include supermassive black hole growth and star accretion during galaxy mergers, and simulating models with different bump parameters. Since a large fraction of the Local Volume is occupied by the Local Void, which may bias luminosity functions, we plan to study luminosity functions in overdense and underdense regions.

7 Acknowledgments

The work of O.R. Skorikov and S.V. Pilipenko was supported by the Basis Foundation grant for theoretical physics and mathematics development. The work of S.A. Drozdov was supported by grant NNG-36-2024.

References

- [1] M. Boylan-Kolchin, J. S. Bullock, and M. Kaplinghat, "Too big to fail? The puzzling darkness of massive Milky Way subhaloes," *MNRAS*, vol. 415, pp. L40–L44, July 2011.
- [2] W. J. G. de Blok, "The Core-Cusp Problem," Advances in Astronomy, vol. 2010, p. 789293, Jan. 2010.

- [3] A. G. Riess, S. Casertano, W. Yuan, J. B. Bowers, L. Macri, J. C. Zinn, and D. Scolnic, "Cosmic Distances Calibrated to 1% Precision with Gaia EDR3 Parallaxes and Hubble Space Telescope Photometry of 75 Milky Way Cepheids Confirm Tension with ΛCDM," Astroph. J. Letters, vol. 908, p. L6, Feb. 2021.
- [4] R. P. Naidu, P. A. Oesch, D. J. Setton, J. Matthee, C. Conroy, B. D. Johnson, J. R. Weaver, R. J. Bouwens, G. B. Brammer, P. Dayal, G. D. Illingworth, L. Barrufet, S. Belli, R. Bezanson, S. Bose, K. E. Heintz, J. Leja, E. Leonova, R. Marques-Chaves, M. Stefanon, S. Toft, A. van der Wel, P. van Dokkum, A. Weibel, and K. E. Whitaker, "Schrodinger's Galaxy Candidate: Puzzlingly Luminous at $z \approx 17$, or Dusty/Quenched at $z \approx 5?$," $arXiv \ e-prints$, p. arXiv:2208.02794, Aug. 2022.
- [5] R. P. Naidu, P. A. Oesch, P. van Dokkum, E. J. Nelson, K. A. Suess, G. Brammer, K. E. Whitaker, G. Illingworth, R. Bouwens, S. Tacchella, J. Matthee, N. Allen, R. Bezanson, C. Conroy, I. Labbe, J. Leja, E. Leonova, D. Magee, S. H. Price, D. J. Setton, V. Strait, M. Stefanon, S. Toft, J. R. Weaver, and A. Weibel, "Two Remarkably Luminous Galaxy Candidates at z ≈ 10-12 Revealed by JWST," Astroph. J. Letters, vol. 940, p. L14, Nov. 2022.
- [6] C. C. Lovell, I. Harrison, Y. Harikane, S. Tacchella, and S. M. Wilkins, "Extreme value statistics of the halo and

- stellar mass distributions at high redshift: are $\langle i \rangle$ jwst $\langle i \rangle$ results in tension with λ cdm?," Monthly Notices of the Royal Astronomical Society, vol. 518, pp. 2511–2520, nov 2022.
- [7] P. Ivanov, P. Naselsky, and I. Novikov, "Inflation and primordial black holes as dark matter," *Phys. Rev. D*, vol. 50, pp. 7173–7178, Dec. 1994.
- [8] K. Inomata, M. Braglia, and X. Chen, "Questions on calculation of primordial power spectrum with large spikes: the resonance model case," *JCAP*, vol. 2023, p. 011, Apr. 2023.
- [9] S. Chabanier, M. Millea, and N. Palanque-Delabrouille, "Matter power spectrum: from Ly α forest to CMB scales," MNRAS, vol. 489, pp. 2247–2253, Oct. 2019.
- [10] M. V. Tkachev, S. V. Pilipenko, E. V. Mikheeva, and V. N. Lukash, "Excess of high-z galaxies as a test for bumpy power spectrum of density perturbations," MN-RAS, vol. 527, pp. 1381–1388, Jan. 2024.
- [11] S. V. Pilipenko, S. A. Drozdov, M. V. Tkachev, and A. G. Doroshkevich, "Galaxies at $z \sim 10$ and New Opportunities for Testing Cosmological Models," Astrophysical Bulletin, vol. 79, pp. 535–547, Dec. 2024.
- [12] M. V. Tkachev, S. V. Pilipenko, E. V. Mikheeva, and V. N. Lukash, "Inner structure of dark matter halos at high z

- in cosmological models with non-powerlaw primordial spectra," *Phys. Rev. D*, vol. 110, p. 083530, Oct. 2024.
- [13] J. Wu, T. K. Chan, and V. J. Forouhar Moreno, "Cosmological zoom-in simulations of Milky Way host mass dark matter halos with a blue-tilted primordial power spectrum," *Phys. Rev. D*, vol. 112, p. 023512, July 2025.
- [14] Y. N. Eroshenko, V. N. Lukash, E. V. Mikheeva, S. V. Pilipenko, and M. V. Tkachev, "Absorption in the 21 cm Hydrogen Line at z > 10 as a Sensitive Tool for the Construction of a Cosmological Model On Small Scales," Astronomy Letters, vol. 51, no. 4, pp. 189–197, 2025.
- [15] E. O. Nadler, V. Gluscevic, and A. Benson, "The Effects of Linear Matter Power Spectrum Enhancement on Dark Matter Substructure," Astroph. J., vol. 993, p. 17, Nov. 2025.
- [16] A. V. Zasov, A. S. Saburova, A. V. Khoperskov, and S. A. Khoperskov, "Dark matter in galaxies," *Physics Uspekhi*, vol. 60, p. 3, Apr. 2017.
- [17] P. G. van Dokkum, R. Abraham, A. Merritt, J. Zhang, M. Geha, and C. Conroy, "Forty-seven Milky Waysized, Extremely Diffuse Galaxies in the Coma Cluster," Astroph. J. Letters, vol. 798, p. L45, Jan. 2015.
- [18] A. Kravtsov and V. Manwadkar, "GRUMPY: a simple framework for realistic forward modelling of dwarf

- galaxies," *MNRAS*, vol. 514, pp. 2667–2691, Aug. 2022.
- [19] A. Dekker and A. Kravtsov, "Constraints on blue and red tilted primordial power spectra using dwarf galaxy properties," *Phys. Rev. D*, vol. 111, p. 063516, Mar. 2025.
- [20] A. Klypin, I. Karachentsev, D. Makarov, and O. Nasonova, "Abundance of field galaxies," MNRAS, vol. 454, pp. 1798– 1810, Dec. 2015.
- [21] E. Hawkins, S. Maddox, S. Cole, O. Lahav, D. S. Madgwick, P. Norberg, J. A. Peacock, I. K. Baldry, C. M. Baugh, J. Bland-Hawthorn, T. Bridges, R. Cannon, M. Colless, C. Collins, W. Couch, G. Dalton, R. De Propris, S. P. Driver, G. Efstathiou, R. S. Ellis, C. S. Frenk, K. Glazebrook, C. Jackson, B. Jones, I. Lewis, S. Lumsden, W. Percival, B. A. Peterson, W. Sutherland, and K. Taylor, "The 2dF Galaxy Redshift Survey: correlation functions, peculiar velocities and the matter density of the Universe," MNRAS, vol. 346, pp. 78–96, Nov. 2003.
- [22] S. Pilipenko, G. Yepes, S. Gottlöber, and S. Knollmann, "Ginnungagap – a massively parallel cosmological initial conditions generator," arXiv e-prints, p. arXiv:2511.10353, Nov. 2025.
- [23] V. Springel, "The cosmological simulation code GADGET-2," MNRAS, vol. 364, pp. 1105–1134, Dec. 2005.

- [24] P. S. Behroozi, R. H. Wechsler, and C. Conroy, "THE AVERAGE STAR FORMATION HISTORIES OF GALAXIES IN DARK MATTER HALOS FROM<i>z</i>= 0-8," The Astrophysical Journal, vol. 770, p. 57, may 2013.
- [25] P. Kroupa, "On the variation of the initial mass function," *MNRAS*, vol. 322, pp. 231–246, Apr. 2001.
- [26] C. Conroy, J. E. Gunn, and M. White, "The Propagation of Uncertainties in Stellar Population Synthesis Modeling. I. The Relevance of Uncertain Aspects of Stellar Evolution and the Initial Mass Function to the Derived Physical Properties of Galaxies," Astroph. J., vol. 699, pp. 486–506, July 2009.
- [27] C. Conroy and J. E. Gunn, "The Propagation of Uncertainties in Stellar Population Synthesis Modeling. III. Model Calibration, Comparison, and Evaluation," Astroph. J., vol. 712, pp. 833–857, Apr. 2010.
- [28] I. D. Karachentsev, D. I. Makarov, and E. I. Kaisina, "Updated Nearby Galaxy Catalog," Astron. J., vol. 145, p. 101, Apr. 2013.
- [29] V. Yankelevich and S. V. Pilipenko, "Towards accurate rescaling of a halo mass function," *Open Astronomy*, vol. 27, pp. 150–156, July 2018.